Influence of Entanglements on the Time Dependence of Mixing in Nonradiative Energy Transfer Studies of Polymer Diffusion in Latex Films

Ewa Odrobina and Mitchell A. Winnik*

Department of Chemistry, University of Toronto, 80 St. George St., Toronto, Ontario, Canada M5S 3H6

Received August 17, 2000; Revised Manuscript Received April 27, 2001

ABSTRACT: We report energy transfer experiments on poly(butyl methacrylate) (PBMA) latex films prepared from a 1:1 mixture of donor- and acceptor-labeled latex particles. In one set of samples, the particles contain low molecular weight polymer ($M_w = 34\,000$) comparable to the entanglement molecular weight (M_e) of PBMA. For this sample, the extent of mixing f_m (defined as the fractional increase in the energy transfer quantum yield) increased with time as $t^{1/2}$, consistent with diffusion that follows Fick's law. In the second set of experiments, involving polymer with $M_w = 380\,000$ ($M_w > 10M_e$), we observe a change in the time dependence of f_m. At early times, for values of $f_m < 0.2$, f_m scales as $t^{1/2}$. There is a sharp crossover to a $t^{1/4}$ scaling relationship for values of $f_m > 0.2$. The most likely explanation of the early-time behavior is Fickian diffusion of the lowest molecular weight components of the broadly disperse polymer ($M_w/M_n = 3$). The scaling of f_m with $t^{1/4}$ does not appear to be consistent with the predictions of the theory of polymer diffusion across interfaces. The parameter f_m is a measure of the number of monomers crossing the interface $N(t)$. For diffusion across a planar interface, $N(t)$ is predicted to increase as $t^{3/4}$ if the chain ends are uniform and as $t^{1/2}$ if they are segregated to the interface.

Introduction

When two pieces of polymer are brought into intimate contact and heated to a temperature above their glass transition temperature T_g, the interface between the polymers gradually disappears, and the strength of the interface increases. The key characteristic of this welding process is that the initial interface serves as a dividing plane, with individual polymer molecules confined to either side of the interface. Annealing promotes polymer diffusion across the interface, and chains that span the interface are the source of adhesion.

The healing of latex films represents a special case of polymer diffusion across interfaces. Here the films are prepared from polymers in the form of spherical particles, similar in size, dispersed in water. When the water dries, the particles are forced into contact. If the polymer T_g is below ambient temperature, the forces associated with drying are sufficient to deform the particles into space-filling polyhedra, with intimate contact between adjacent cells. As in the welding experiment described above, the newly formed interfaces are weak, and strong adhesion evolves through polymer diffusion across the intercellular boundaries. There are two major differences between the welding of two polymer slabs and the evolution of latex film properties. The first is that, from the point of view of an individual cell, polymer diffusion occurs with spherical symmetry in the latex film. In addition, latex particles are normally prepared by emulsion polymerization and, as a consequence, contain polymers with a rather broad distribution of molecular weights ($M_w/M_n \approx 2-3$).

In this paper we report a simple scaling relationship between the "extent of mixing", as determined in a fluorescence energy transfer (FRET) experiment, and the annealing time for the diffusion of entangled polymers in latex films. This result is important because it involves the diffusion of polymer molecules across the intercellular boundaries in the latex film. The result is unexpected, because it appears from our perspective not to correspond to any of the predictions of the theory of polymer diffusion across interfaces. Polymer diffusion in latex films has also been studied by small-angle neutron scattering (SANS). While the information available from SANS is different than that available from FRET, recent SANS experiments on films prepared from polystyrene nanospheres are largely consistent with the predictions of theory. It thus becomes important to try to understand the differences in the results obtained by these two techniques.

We begin our report with a brief overview of the theory of polymer diffusion across interfaces, followed by a comparison of the information available from SANS and FRET experiments on latex films. After a brief Experimental Section, we describe our results and then comment on the features of our experiment that may lead to the results we obtain.

Polymer Diffusion across Interfaces. Polymer diffusion is driven by Brownian motion and consists of random thermal jumps of segments of polymer chains between adjacent voids or "free volume elements". Two models, the Rouse model[1] and the reptation model,[2] are commonly employed to describe self-diffusion of polymer chains in the melt state. The Rouse model takes account of the effect of chain connectivity on the friction coefficient of a diffusing chain. This model assumes that each polymer chain consists of N beads connected by $(N - 1)$ springs, and each bead feels the same friction f from the surrounding media. This model provides a normal-mode description of the polymer dynamics, characterized by a distribution of relaxation times. The longest relaxation time τ_{ro} is often referred to as the Rouse time. When the molecular weight of polymer is

* Corresponding author. E-mail mwinnik@chem.utoronto.ca.

10.1021/ma0014618 CCC: $20.00
Published on Web 07/14/2001

not too high, $M < 2M_e$ (M_e is the critical entanglement molecular weight), the Rouse model can be used to describe the translational diffusion of polymer molecules.

The reptation model adds topological (entanglement) effects to the description of chain dynamics for high-M polymers, where entanglements influence the polymer dynamics. In this model, neighboring chains are obstacles, restricting the lateral motion of a polymer chain and confining the chain to a "tube" where curvilinear, one-dimensional diffusion occurs along its contour. Random motion occurs in both directions along the tube. Memory of the initial chain conformation (tube conformation) is gradually lost because the motion of the chain ends is random. Finally, after a reptation time T_{rep}, a chain disengages itself from the initial tube and takes a new conformation. At times much shorter than T_{rep}, the Rouse model is employed to describe the relaxation of the chain confined to its tube.

For polymer diffusion across an interface, one has to take into account the influence of the interface as a dividing plane on the initial chain conformation.[3−6] Prior to the onset of diffusion, the conformation of the polymer chains close to the interface is distorted from the normal Gaussian distribution of segments typifying polymer chains in the bulk state. This distortion is referred to as confinement entropy. The diffusion of polymer molecules across the interface leads to conformational randomization and recovery of Gaussian chain statistics. For short chains, in which translational diffusion can be described by the Rouse model, the chain relaxation time at the interface is very short, and polymer diffusion follows Fick's[6,7] laws. For entangled chains, the process is substantially more complex. According to the reptation model, the diffusion process is dominated by segmental motion for times shorter than T_{rep}, whereas center-of-mass diffusion prevails at longer times.

The theory of polymer diffusion across interfaces for entangled chains[3−6] predicts that the diffusion will follow Fick's law when the diffusion time is larger than the reptation time (T_{rep}). In this case, the mass transfer scales with time as $t^{1/2}$. The interesting predictions are those that pertain to reptation dynamics at $t < T_{rep}$. The properties examined include the number of chains crossing the interface $n(t)$, the number of bridges crossing the interface $p(t)$, the number of monomers crossing the interface $N(t)$, and the average monomer penetration depth $X(t)$.[6] Under some circumstances, one might imagine a tendency for segregation of the chain ends at the interface. Under these circumstances, the time evolution of some of these properties (the average contour length of the chain, the average monomer penetration distance $X(t)$, and the average bridge length) are unaffected, whereas the number of chains $n(t)$, the number of bridges $p(t)$, and the number of monomers $N(t)$ crossing the interface have different scaling laws. We are particularly interested in $X(t)$ and $N(t)$. We summarize the predictions for the time-scaling behavior of these quantities for times $t < T_{rep}$ and $t > T_{rep}$ in Table 1.

Table 1. Scaling Law Predictions for the Time Dependence of Polymer Diffusion across an Interface

property	location of chain ends	$t < T_{rep}$	$t > T_{rep}$
penetration depth[a]	random	$t^{1/4}$	$t^{1/2}$
	interface	$t^{1/4}$	$t^{1/2}$
no. of monomers $N(t)$	random	$t^{3/4}$	$t^{1/2}$
	interface	$t^{1/2}$	$t^{1/2}$

[a] For a planar geometry, the penetration depth is referred to as $X(t)$; for radial diffusion in a spherical geometry, we use the term $d = d(t)$.

For the case of a flat distribution of chain ends in the two polymer slabs brought together to form the interface, the most profound prediction is that the monomer concentration of chains crossing the interface is discontinuous for healing times shorter than the reptation time. The gap occurs because there are regions of the interface plane at $t < T_{rep}$ that have not yet been threaded by reptating chains. As the number of chains crossing the interface increases, the gap decreases, and the discontinuity becomes smaller. The gap is predicted to disappear at $t = T_{rep}$.

The basis for these predictions and a much deeper analysis of the theory of polymer diffusion across interfaces is presented in the monograph by Wool.[6] A more complete picture of the evolution of polymer segment density at the interface has to take into account contributions of small scale displacements of individual segments, larger amplitude Rouse-type relaxation of the polymer backbone between entanglements, the long-time Rouse relaxation of the polymer chain within the tube, and finally reptation diffusion. These processes make their dominant contribution to the diffusion process at different times. Segmental motion occurs on the time scale τ_o of a local jump process and is independent of molecular weight. Polymer segments between entanglements undergo lateral displacements on a time scale characterized by the Rouse time of the entanglement length, τ_e. Over this time period, the monomer diffusion distance is of the order of the radius of gyration of the entanglement chain with molecular weight M_e. Both of these processes increase the number of monomers that cross the interface at early times and soften the discontinuity in the distribution of monomers in chains crossing the interface at $t \ll T_{rep}$. At longer times less than T_{rep}, polymer relaxation along the tube contour is governed by the Rouse relaxation of the chain, whereas in the lateral direction, the chains cannot diffuse farther than the tube wall.

Techniques for Studying Polymer Diffusion across Interfaces. The most powerful methods for studying polymer diffusion across interfaces involve techniques that examine samples with a sandwich geometry with intimate contact between two thin polymer films. One of the many advantages of these methods is that these films can be prepared from polymers with a narrow molecular weight distribution. Thus, molecular weight relationships predicted by the theory can be examined. Contrast is obtained by selective deuteration of one of the films. The dynamic secondary ion mass spectroscopy (SIMS) experiment has a resolution of about 10 nm and makes no specific assumptions about the shape of the monomer concentration profile that evolves through diffusion.[8] Specular neutron reflectivity (SNR) experiments provide even richer information with higher resolution, but the data analysis requires one to assume a shape for the polymer segment density profile across the interface.[9]

A number of elegant experiments have been reported over the past 15 years on such samples.[8,9] It is perhaps not surprising that almost all of the results are for polystyrene, for which a large range of samples of different molecular weights are available. The results of these experiments are in good accord with the

predictions of the theory and provide little evidence for the idea that the chain ends are enriched in the interface.

For latex films, diffusion occurs with spherical symmetry. For such systems, we have fewer experiments on fewer well-defined systems, and the range of techniques that one can employ is more limited than for the study of thin polymer films. While Fick's laws of diffusion can easily be evaluated in spherical geometry, the corresponding laws governing reptative diffusion across interfaces have not been derived for a spherical geometry. The two techniques that have been applied to study diffusion in latex films are SANS and FRET.

Studying Latex Films by Neutrons and Photons. In a SANS experiment, the major source of contrast is provided by the difference in scattering cross sections of protons and deuterons. To study polymer diffusion in latex films, one prepares films in which a small fraction of the latex particles contain deuterated polymer. In the FRET experiment, contrast is provided by the use of two different fluorescent dyes, a donor dye D and an acceptor dye A. In this experiment, D is selectively excited with light, and its excited state (D*) can transfer energy to A through a mechanism involving resonant coupling of the transition dipoles. The level of dye incorporation is on the order of 1 mol %. To study polymer diffusion in latex films, one prepares films in which some of the latex particles contain polymer covalently labeled with D, and the rest of the latex particles contain polymer labeled with A. In a scattering experiment, one measures the angular dependence of the scattering intensity I_s, and one plots log I_s vs the scattering vector q. In the FRET experiment, one excites the sample with a short pulse of light and measures the time dependence of the donor intensity decay $I_D(t')$ and then plots log $I_D(t')$ vs t'. In describing these experiments, we distinguish the fluorescence decay time t' from the sample annealing time t.

In both experiments, the latex films are prepared in a similar way. The two dispersions are mixed, and the mixture is drawn down to form a film. If the latex polymers are sufficiently soft, the particles will undergo deformation into space-filling polyhedral cells during the drying process. If the particles are too hard to deform in this way, one obtains a mixed powder that can be compression molded with the application of heat into similar films consisting initially of space-filling polyhedral cells. One begins by carrying out a measurement on the nascent film representing the state of intimate contact between adjacent cells in which little or no polymer diffusion has taken place. One then anneals the films for various times to promote polymer diffusion. The sample is then cooled or frozen to stop diffusion while the measurement is repeated. The sample is put back in the oven to continue the annealing process. One repeats the measurement as a function of annealing time.

The data provided by these two very different experiments have interesting features in common. The plot of scattering intensity vs scattering vector q, like the plot of $I_D(t')$ vs t', represents a snapshot of the system at a given annealing time. For latex films, both are monotonic and featureless "decay" profiles. To obtain the diffusion coefficient characterizing the polymer diffusion, one has to introduce a theoretical segment density distribution, based upon a model for the diffusion mechanism, into the analysis of the intensity profile. It is also possible to analyze the data in a model-free way. In the SANS experiment, one can calculate the radius of gyration R_G through a Guinier analysis of the intensity profile. In the ET experiment, one can calculate the quantum efficiency of energy transfer Φ_{ET} from the integrated donor intensity decay profile. In the following paragraphs, we describe in more detail these "minimum-assumption" approaches to analyzing the experimental data.

Chart 1. Monitoring Polymer Diffusion in a SANS Experiment

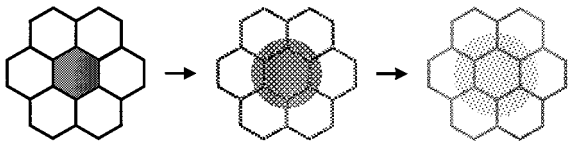

When polymer diffusion is studied by SANS, one examines a film in which isolated cells of deuterated polymer are encased in a matrix of cells of nondeuterated polymer. A drawing describing the essential features of this experiment is shown in Chart 1. The gray hexagon in the center of the drawing represents a cross section of a cell formed from a particle consisting of deuterated polymer. The lines represent the boundaries of the cells, where polar material (salt, surfactant, polar groups) from the latex surface tends to be trapped in the newly formed film. As the film is heated, the polymer molecules begin to diffuse, and one monitors the diffusion of the deuterated polymer molecules out of their initial cell. In the Guinier analysis of the SANS intensity profile, one determines the growing radius of gyration of the object defined by the deuterated polymer as it diffuses away from its initial cell. In principle, one can continue to obtain information about diffusion in this experiment until the positions of the individual polymer molecules become uncorrelated. The information one obtains is the average diffusion distance or penetration depth as a function of annealing time.

The first experiments on latex films involving SANS, reported by Hahn and Ley,[10] examined the diffusion of deuterated poly(butyl methacrylate) (PBMA-d) in a matrix of nondeuterated polymer. Sperling and Klein[11,12] used SANS to follow polymer diffusion in compression-molded films prepared from polystyrene latex powder. Their most impressive results come from studies of "artificial" latex particles prepared by emulsifying polystyrene of narrow molecular weight distribution. They compared the extent of polymer diffusion with the growth of tensile strength in latex films. They found that the mechanical strength of the film increases with diffusion and reaches a maximum value as the polymer molecules diffuse a distance equal to one radius of gyration (R_g) across the interface. More recently, Joanicot et al.[13] have used SANS measurements to follow polymer diffusion in poly(styrene-*co*-butyl acrylate) latex films.

In the ET experiment, one monitors the diffusion across the boundary between donor-labeled cells and acceptor-labeled cells. A drawing describing the essential features of this experiment is shown in Chart 2. The film consists of a mixture of cells formed from donor- and acceptor-labeled latex particles. In the initial film, the D and A groups are confined to their respective cells. The characteristic distance R_0 for ET is on the order of tens of angstroms, much smaller than the cell dimensions (typically 50−100 nm). In the newly formed

Chart 2. Monitoring Polymer Diffusion in an ET Experiment

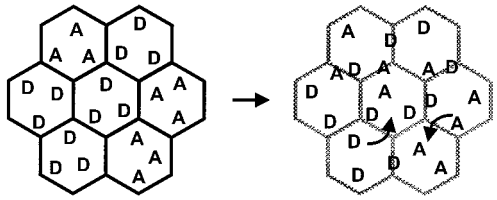

film, one can measure a small amount of ET between D* groups in one cell and A groups in the adjacent cell. The extent of the interfacial ET is sensitive to the ratio of D- and A-labeled particles in the blend. In principle, the magnitude of the quantum efficiency of ET (Φ_{ET}) at this point measures the amount of interfacial area between D- and A-labeled cells. As the film is annealed, polymer diffusion occurs. The polymers carry with them their covalently bound dyes. When polymer diffusion occurs across the boundary between a cell consisting of donor-labeled polymer and that containing acceptor-labeled polymer, there is an increase in the number of D and A groups in proximity. As a consequence, the magnitude of Φ_{ET} evolves from its initial value $\Phi_{ET}(0)$ to that characteristic of a homogeneously mixed film $\Phi_{ET}(\infty)$.

The evolution of Φ_{ET} as a function of annealing time t can be used to calculate the extent of mixing of the two labeled polymers.

$$f_m = \frac{\Phi_{ET}(t) - \Phi_{ET}(0)}{\Phi_{ET}(\infty) - \Phi_{ET}(0)} \quad (1)$$

where f_m is defined in terms of the evolution of the quantum efficiency of energy transfer. These values of f_m are only indirectly related to the fraction of mass f_s that has diffused across the interface.[14−16]

For more than a decade, we have employed FRET experiments to study polymer diffusion in latex films. Most of the systems we examined involved linear PBMA and its copolymers. We have employed this techniques to evaluate the influence of external variables such as temperature, plasticizers, surfactant, moisture, and filler particles on the rate of polymer diffusion. The use of ET to study polymer diffusion in latex films has also been reported by Boczar et al.[17] and by the Lang group[18] in France.

In this paper we examine the dependence of f_m on annealing time t for low and high molecular weight PBMA samples and note that for PBMA $M_e \approx 30\,000$.[19] For low molecular weight samples, with $M_w \approx M_e$, f_m has a power law time dependence and scales as $t^{1/2}$. For the high molecular weight sample, with $M_w > 10M_e$, we find that f_m increases as $t^{1/4}$. Closer inspection of the data reveals that, at early times for these high molecular weight samples, f_m increases as $t^{1/2}$, with a subsequent crossover to a $t^{1/4}$ dependence. Some of the data we describe were obtained in a series of experiments intended to examine the influence of small soft cross-linked polymer particles on the polymer diffusion rate. These experiments will be described in detail elsewhere.[20] For the purposes of this paper, we note only that increasing amounts of soft filler acts to retard the growth in time of f_m. The presence of filler does not seem to affect the crossover in scaling of f_m at $f_m \approx 0.2$ from $t^{1/2}$ to $t^{1/4}$ scaling. These samples provide additional examples of this unusual change in the time course of the intercellular polymer diffusion in latex films.

Table 2. Recipe for the Preparation of Labeled PBMA Latex

first stage		second stage	
BMA (mL)	3.3	BMA (mL)	30
DM (mL)	0 or 0.074[a]	DM (mL)	0 or 0.68[a]
water (mL)	60	PheMMA[b] (g)	0.58
KPS (g)	0.066	water (mL)	24
SDS (g)	0.099	KPS (g)	0.06
$NaHCO_3$ (g)	0.066	SDS (g)	0.54
temp (°C)	80	temp (°C)	80
time (h)	1	time (h)	20−24

[a] For preparation of high M PBMA, no chain transfer agent was added; for preparation of low-*M* PBMA, 0.68 mL of *n*-dodecyl mercaptan was used. [b] When using 9-vinyl phenanthrene (V-Phe) as the dye comonomer, this quantity becomes 0.48 g. For preparing the An-labeled latex, 0.62 g of (9-anthryl) methacrylate (AnMA) was used to replace 0.58 g of (9-phenanthryl) methyl methacrylate (PheMMA).

Table 3. Characteristics of the Latex Particles

high *M*[a]	M_w (g/mol)	M_n (g/mol)	*d* (nm)	T_g (°C)	dye content (mol %)
Phe-PBMA	380 000	130 000	124 (0.034)[b]	34	0.9
An-PBMA	420 000	130 000	132 (0.024)[b]	34	0.9
low M[a]					
Phe-PBMA	35 000	16 000	120 (0.028)[b]	21	0.9
An-PBMA	34 000	17 000	120 (0.032)[b]	21	1.0
PBA microgel particles[c]			56	−43	

[a] For all PBMA samples the molecular weights were determined by gel permeation chromatography (GPC, with poly(methyl methacrylate) standards). [b] Size polydispersity. [c] 1,6-Hexanediol diacrylate (3.75 wt % based on BA monomer weight) was used as a cross-linking agent.

Experimental Section

Materials. Polymer diffusion experiments were carried out on dye-labeled PBMA samples of both high molecular weight ($M_w = 4 \times 10^5$) and low molecular weight ($M_w = 3.5 \times 10^4$) PBMA. Both sets of polymers had $M_w/M_n = 2.5-3.5$ and a degree of labeling of 0.9−1.0 mol %. Phenanthrene (Phe)- and anthracene (An)-labeled PBMA aqueous latex particles with diameters of ca. 140 nm were prepared at 30 wt % solids by conventional emulsion polymerization using a procedure similar to that reported previously.[21] Film samples were prepared from a 1:1 mixture of donor- and acceptor-labeled latex particles, referred to here as Phe-PBMA and An-PBMA, respectively. These particles were prepared to be matched as closely as possible in molecular weight, molecular weight distribution, and particle size. To help control these features of the reaction, both semicontinuous emulsion polymerization reactions were run under strictly identical conditions, using a common unlabeled seed latex. The recipes employed in the syntheses of the latex dispersions are presented in Table 2, and the characteristics of the latex particles are presented in Table 3. These dispersions were purified by ion exchange (Bio-Rad, AG-501-X8 mixed bed resin, 3 g of resin per 100 mL of latex) to remove surfactant and low molecular weight salts used in the preparation of the latex dispersions. The procedure was repeated three times.

In some experiments, known aliquots of fully cross-linked poly(butyl acrylate) (PBA) microgel particles were added to the dispersion of the mixture of the Phe- and An-labeled latex particles. The preparation and characterization of these particles will be reported elsewhere.[20] Their characteristics are also given in Table 3.

Sample Preparation. Latex films were prepared from a mixed dispersion containing a 1:1 number ratio of Phe- and An-labeled PBMA particles. The mixtures of latex dispersions

were gently shaken for 10 min and then cast onto quartz slides. The plates were covered with an inverted Petri dish and placed in an oven for about 4 h to form dry, crack-free, and transparent films. The film formation temperature was 34 °C for the high-*M* PBMA samples and 22 °C for the low-*M* PBMA. After the films were dry, they were annealed at 55 °C (low-*M* PBMA) and at 70 and 76 °C (high-*M* PBMA). The thickness of the films was in the range 30−50 μm.

Some PBMA films contained fully cross-linked poly(butyl acrylate) (PBA) latex particles as a filler with the volume ratio of 10, 30, and 60% PBA. In this case PBA particles were added to PBMA latex dispersion. The mixtures of latex dispersions were gently shaken for 10 min and then cast onto quartz plates and allowed to dry as described above.

Fluorescence Decay Measurements. All fluorescence decay profiles were measured by the time-correlated single-photon counting technique.[22] The measurements were conducted at room temperature. The donor phenanthrene was excited at 296 nm, and its emission was recorded at 350−360 nm. A band-pass filter (320−390 nm) was mounted in the front of the photomultiplier tube detector to minimize the interference due scattered light and from the fluorescence of excited acceptors. For fluorescence decay measurements, each sample was placed in a small quartz test tube and kept under a nitrogen atmosphere during the measurement. In the case of annealed samples, before measurements, they were removed from the oven and cooled to room temperatures. Finally, the fluorescence decay profiles were measured, and the areas under each decay curve were integrated and analyzed as described below.

A useful measure of the extent of energy transfer (ET) in the system is the quantum efficiency of energy transfer Φ_{ET}, which we calculate from the donor fluorescence decay profiles $I_D(t')$ for films in the presence and absence of acceptor.

$$\Phi_{ET} = 1 - \frac{\int_0^\infty I_D(t')\,dt'}{\int_0^\infty I_D^0(t')\,dt'} = 1 - \frac{\text{Area}(t)}{\text{Area}([An] = 0)} \qquad (2)$$

The middle term represents the definition of the energy transfer efficiency in terms of the integrated intensity decays profiles, where $I_D^0(t')$ is the donor decay profile in the absence of acceptor. For latex films containing phenanthrene as the donor, $I_D^0(t')$ is always exponential. Area(t) represents the integrated area under the fluorescence decay profile of a latex film sample annealed for a time t, and Area([An] = 0) refers to the area under the decay profile of a film containing only donor. To calculate these areas, nonexponential decay profiles are fitted to the stretched exponential in eq 3.

$$I_D(t') = B_1 \exp\left[-\frac{t'}{\tau_D} - P\left(\frac{t'}{\tau_D}\right)^{1/2}\right] + B_2 \exp\left(-\frac{t'}{\tau_D}\right) \qquad (3)$$

The fitting parameters B_1, B_2, and P in eq 3 obtained from each profile are useful for area integration, but their physical meaning is not important here. These integrated areas have dimensions of time and define an average decay time $\langle\tau_D\rangle$ for the sample. We note that the characteristic (Förster) energy transfer distance for Phe and An in PBMA films is 23 Å.[23]

Results and Discussion

A PBMA latex film containing only phenanthrene (Phe) exhibits an exponential fluorescence decay with a lifetime τ_D of 45 ns. Latex films prepared from a 1:1 mixture of donor- and acceptor-labeled PBMA latex, with Phe as the donor and anthracene (An) as the acceptor, show small deviations from a strictly exponential decay profile. The integrated area under this decay gives a mean decay time $\langle\tau_D\rangle = 42$ ns, corresponding to $\Phi_{ET}(0) = 0.07$. Since little or no polymer diffusion takes place at room temperature in our samples, we attribute this difference to trans-boundary energy transfer prior to the onset of polymer diffusion.[24,25] When these films are heated for various periods of time, cooled to room temperature, and reexamined, the samples exhibit nonexponential donor fluorescence decay profiles because of direct nonradiative energy transfer from Phe to An in the films. These decay profiles were fitted to eq 3 and then integrated to obtain the areas corresponding to the different annealing time. Energy transfer efficiencies were calculated, eq 2, and from these, values of f_m, eq 1, were evaluated. Examples of various decay curves are shown in Figure 1.

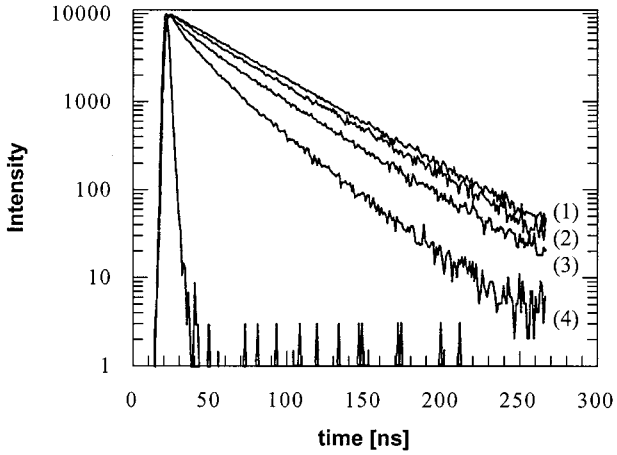

Figure 1. Examples of fluorescence decay curves for PBMA films: (1) containing only phenantrene (Phe); (2) for a freshly formed film containing Phe as the donor and An as the acceptor with a ratio of Phe/An = 1:1; (3) for the same film as in (2) but annealed at 80 °C for 4 h; (4) for the same film as in (2), but fully mixed.

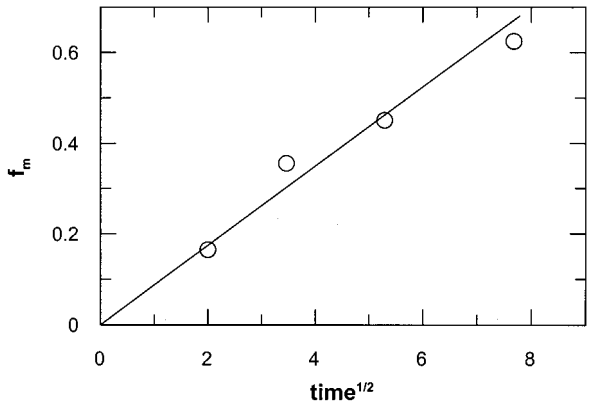

Figure 2. Plot of f_m vs $t^{1/2}$ (f_m is the extent of mixing, and t is the annealing time) for a low molecular weight ($M_w = 3.5 \times 10^4$) PBMA latex film, annealed at 60 °C. In this and all other figures, time is measured in minutes.

FRET Experiments on Low-*M* PBMA Samples. We begin with an examination of the films prepared from the low molecular weight polymer latex particles. For these samples, $M_w = 35\,000$ and $M_w/M_n = 2.2$. In Figure 2, we show the results for one such film annealed at 60 °C and plot f_m against $t^{1/2}$. The plot is linear, and the data range from f_m values of 0.2 to 0.7. To emphasize the power law relationship, we replot these data as (ln f_m) vs (ln t) in Figure 3 and provide examples of two additional film samples prepared from the same latex but annealed separately. The dependence is linear with an average slope of 0.44. This behavior, with f_m scaling with time as $t^{1/2}$, is consistent with diffusion across the cell boundary that satisfies Fick's law.

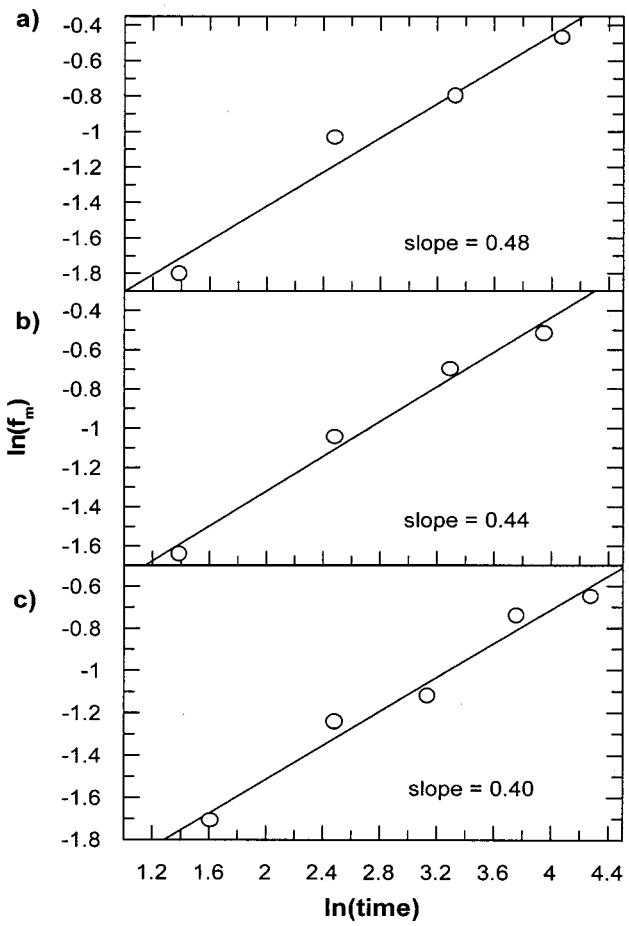

Figure 3. Plots of $\ln(f_m)$ vs $\ln(t)$ for a sample from Figure 2 (a) and two additional film samples prepared from the same latex but annealed saparately (b and c).

It is important to recall that f_m describes the fractional growth in energy transfer efficiency as a consequence of polymer diffusion and not the fractional mass transfer f_s. Farinha et al.[14] have examined the relationship between f_m and the fraction of mass transfer f_s through comparison of simulated donor fluorescence decay profiles. The simulations involved rigorous coupling of the concentration profiles generated through Fickian diffusion with the theory of energy transfer in restricted geometries. Excited donor survival probabilities were then convoluted with an experimental excitation profile followed by the addition of Poisson noise to the signal. In this way they generated $I_D(t)$ decay curves for diffusion in spherical symmetry characterized by a diffusion coefficient of magnitude D_s. At various stages of the simulated diffusion process, the simulated decay curves were integrated (eq 2) to obtain Φ_{ET} values, which were then used to calculate values of f_m. Values of f_s were calculated directly from the simulated concentration profiles. The parameters chosen for this simulation (particle size, acceptor concentration) are very similar to those of the experiments we report here. The authors found a linear dependence of f_m and f_s on $t^{1/2}$ for f_m values up to 0.7 and for f_s values up to 0.6. At this level of acceptor concentration, f_m increased more rapidly than f_s, with $f_m = 0.7$ corresponding to $f_s = 0.45$. Thus, as about half the mass of the original 100 nm diameter donor-labeled sphere has diffused into the surrounding matrix, the FRET experiment begins to lose sensitivity.

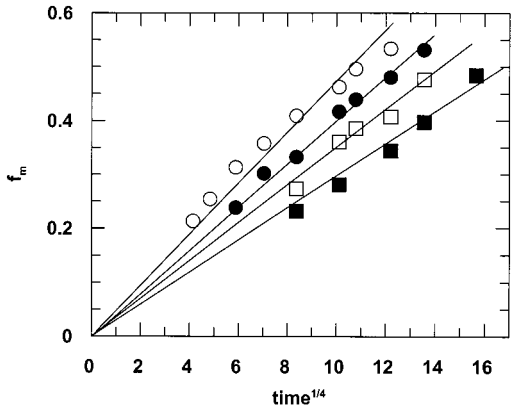

Figure 4. Plots of f_m vs $t^{1/4}$ for the high molecular weight ($M_w = 4 \times 10^5$) PBMA sample and its blends, annealed at 70 °C: (○) in the absence of presence of cross-linked poly(butyl acrylate) (PBA) microspheres, (●) 10 vol % PBA, (□) 30% PBA, (■) 60% PBA. The data in this figure are limited to $f_m > 0.2$.

It is important to emphasize here that the proportionality constant between f_s and f_m depends on the acceptor-dye concentration in the A-labeled particles.[25] Thus, experiments with different samples can be compared only if the level of acceptor labeling is kept constant. We have reported a number of experiments for PBMA latex films in which the polymer $M_w < 2M_e$ and the acceptor-dye concentration in the A-labeled particles was similar to that reported here. For all of these films, we found that f_m increased in proportion to $t^{1/2}$ for values up to $f_m \approx 0.7$. Under these circumstances, we have assumed that the diffusion was Fickian and calculated apparent diffusion coefficients (D_{app}) by assuming that $f_m \approx f_s$. Simulations show that the D_{app} values calculated in this way are proportional to the true diffusion coefficients. Thus, the influence of factors that affect the rate of polymer diffusion in latex films, such as a change of temperature or the presence of a plasticizer, can be evaluated.

Apparent diffusion coefficients calculated in this way are averaged over the fraction of polymer that has undergone mixing and has contributed to f_m. When the latex particles contain polymers with a broad distribution of molecular weights, the fastest diffusing species make the largest contributions to f_m at early times. Less mobile polymers make their contribution to f_m at later times. As a consequence, D_{app} values are found to decrease as a function of time and as a function of f_m. For different samples, D_{app} values can meaningfully be compared only at identical extents of mixing.[26]

FRET Experiments on High-*M* PBMA Samples. For the high molecular weight latex samples ($M_w \approx 4 \times 10^5$, $M_w/M_n = 3$), we obtained different results. When we first examined this sample, annealed at 76 °C, we found that f_m increased as $t^{1/4}$. A plot of f_m against $t^{1/4}$ is shown in Figure 4. The $t^{1/4}$ dependence for high molecular weight latex polymers is very reproducible, and others in our laboratory made a similar observation for a high molecular weight PBMA polymer several years ago.[26] In some of these experiments, we find that the first data point sometimes did not fit the line. To obtain reliable data for early diffusion times, we reduced the annealing temperature to 70 °C. Under these circumstances, we find that data points for values of $f_m < 0.2$ do not fit the $t^{1/4}$ line passing through the points at higher values of f_m. Instead, at early times, f_m appears to increase in proportion to $t^{1/2}$, crossing over at later

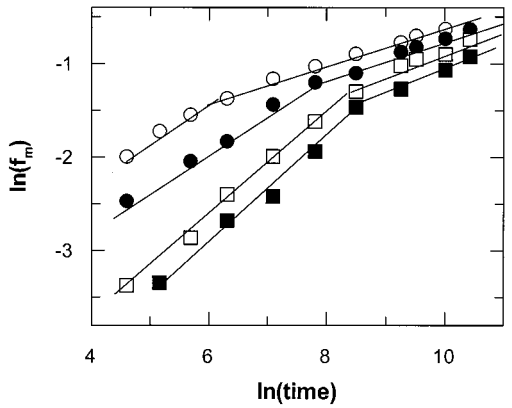

Figure 5. Plots of $\ln(f_m)$ vs $\ln(t)$ (f_m is the extent of mixing, and t is the annealing time) for high molecular weight ($M_w = 4 \times 10^5$) PBMA sample and its blends, annealed at 70 °C: (○) in the absence of presence of cross-linked poly(butyl acrylate) (PBA) microspheres, (●) 10 vol % PBA, (□) 30% PBA, (■) 60% PBA.

times to a $t^{1/4}$ dependence. This crossover is seen clearly when we plot the data logarithmically. The top line in Figure 5 shows two linear portions with a clear break in the vicinity of $f_m \approx 0.2$. The extent of mixing appears to increase as $t^{1/2}$ for the early stages of diffusion, up to $f_m \approx 0.2$, and as $t^{1/4}$ for $f_m > 0.2$.

A word of explanation is in order about why we have in the past missed this crossover. The rate of polymer diffusion increases rapidly with an increase in temperature in accord with the predictions of the Williams−Landel−Ferry (WLF)[27] description of polymer properties coupled to large-amplitude motion of the polymer backbone. For PBMA, over this range of temperatures, the apparent activation energy for polymer diffusion is 160 kJ/mol. Normally, we choose the annealing temperature in such a way that we are able to monitor the entire diffusion process over a reasonably short period of time (a maximum of a few days). The shortest annealing time we can measure and still allow time for the sample to equilibrate in the oven is 15 min. Under these circumstances, we obtain at most two values of f_m in the range of $0 < f_m < 0.2$. Here we are more patient. By lowering the annealing temperature, we measured four to six data points in the region $0 < f_m < 0.2$, and by continuing these measurements over a period of weeks, we obtained additional data for f_m in the range 0.2−0.7. Only in this way it is possible to obtain sufficient data points to identify the crossover from $t^{1/2}$ to $t^{1/4}$ dependence in the polymer diffusion process.

These experiments with the higher molecular weight sample were repeated on latex films which contained 10−60 vol % of small cross-linked poly(butyl acrylate) (PBA) particles. One can see from the data in Figure 4 that increasing amounts of these particles in the film retard the intercellular diffusion of PBMA polymer. A full description of those experiments and the influence of soft fillers on polymer diffusion in latex films will be reported elsewhere.[20] Here we use these data to examine the time profile of the growth in f_m. The data for each of the samples fits nicely to two intersecting straight lines. The crossover occurs at approximately $f_m \cong 0.2-0.22$ [$\ln(0.2) = -1.61$, $\ln(0.22) = -1.51$].

In Figure 6 we present an expanded view of the linear dependence of ($\ln f_m$) on ($\ln t$) using the data taken from Figure 5. In Figure 6a we show data for the region with $f_m \leq 0.2$, and in Figure 6b we show the data for the

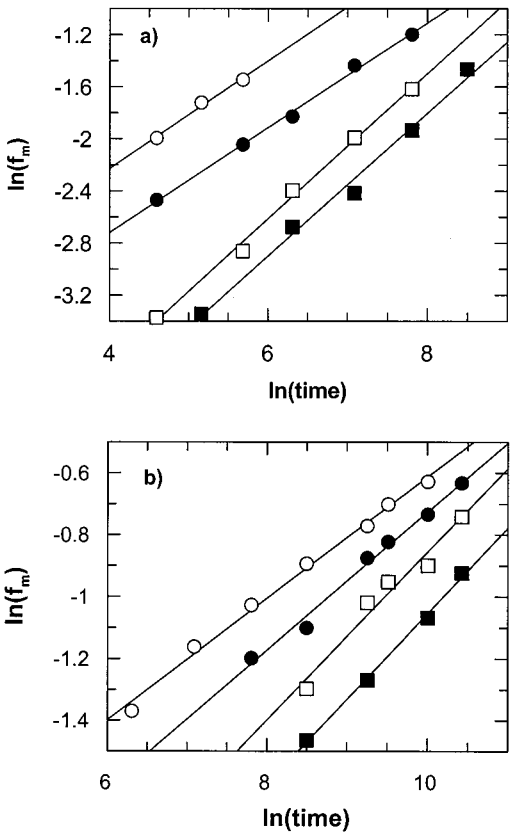

Figure 6. Plots of $\ln(f_m)$ vs $\ln(t)$ for samples from Figure 5: (a) expanded region for $f_m \leq 0.2$, (○) pure PBMA (slope = 0.41), (●) 10 vol % PBA (slope = 0.4), (□) 30% PBA (slope = 0.56), (■) 60% PBA (slope, 0.55); (b) expanded region for $f_m > 0.2$, (○) pure PBMA (slope, 0.20), (●) 10% PBA (slope, 0.22), (□) 30% PBA (slope, 0.27), (■) 60% PBA (slope, 0.28).

Table 4. Values of the Slopes of the Plots of ($\ln f_m$) vs ($\ln t$) for the High Molecular Weight PBMA Sample in the Absence and Presence of Cross-Linked 60 nm PBA Particles

sample	$f_m < 0.2$	$f_m > 0.2$
PBMA	0.41	0.2
PBMA+ 10% PBA	0.4	0.22
PBMA + 30% PBA	0.56	0.27
PBMA + 60% PBA	0.55	0.28

region with $f_m > 0.2$. The data show some scatter in the slopes, and the individual values are collected in Table 4. For early stages of the interdiffusion, the average of the four slopes is 0.47. For later stages of the diffusion, the slope in the absence of filler is equal to 0.25.

Putting the Results in Perspective. *Scaling Relationships.* In designing the energy transfer experiment, we take care to ensure that the dyes are randomly attached to the latex polymer. As a consequence, it is reasonable to assume that the increase in proximity of the donor and acceptor dyes as measured by the increase in Φ_{ET} is a measure of the mixing of monomer units of the polymers originally confined respectively to the donor- and acceptor-labeled cells in the latex film. In terms of comparing results with the predictions of the theory of polymer diffusion across interfaces, we expect f_m and $N(t)$ to follow identical scaling relationships with time. For the low molecular weight polymer sample, the proportionality between f_m and $t^{1/2}$ is consistent with the idea that polymer diffusion in these samples follows Fick's law.

For the high molecular weight polymer at early times, there are several possible explanations for the $t^{1/2}$ dependence. First, lateral diffusion over distances up to a tube diameter will lead to some mixing of donor- and acceptor-labeled polymer. The $t^{1/2}$ scaling relationship may also point to a Fickian contribution to the diffusion process. These polymers have a broad molecular weight distribution ($M_w = 4 \times 10^5$, $M_w/M_n = 3$). The gel permeation chromatography trace (GPC) for this polymer is symmetric but shows a significant component with $M < 10^5$. Since the species that diffuse the fastest contribute to the ET signal at early times, this fraction of the polymer composition may dominate the power law behavior of f_m prior to the crossover. From this perspective, we imagine that the low molecular weight component of the latex polymer diffuses according to Fick's law.

At longer diffusion times, the diffusive mixing of high molecular weight polymer starts to dominate the energy transfer measurements. Here entanglement effects influence the polymer mobility. In our experiment, as a consequence of the influence of entanglements, the dependence of the f_m parameter on time changes from $t^{1/2}$ to $t^{1/4}$. This result is rather different than the prediction for $N(t)$ shown in Table 1. For a random distribution of chain ends (in a planar geometry), $N(t)$ is predicted to increase as $t^{3/4}$, whereas for chain ends localized at the interface, $N(t)$ should scale as $t^{1/2}$.

To put these results in context, we compare them with the SANS results of Kim, Sperling, and Klein,[28] who used an emulsification procedure to prepare spherical polystyrene particles from monodisperse polystyrene (PS-h) and deuteriopolystyrene (PS-d). In their samples, M_n values ranged from 150 000 to 200 000 with $M_w/M_n \leq 1.03$. They mixed particles containing PS-d with a much larger number of similar sized particles containing PS-h and prepared films by compression molding the powder. Polymer diffusion process across the particle−particle interface was monitored by SANS measurements as a function of annealing time. They employed a Guinier analysis of the scattering intensity profiles to determine the radius of gyration $R_g(t)$ of the deuterated domains as polymer diffused out of its initial cell. The authors estimated the penetration depth of the deuterated polymer by taking the difference between the radius of gyration evaluated after the sample was annealed and the initial radius R of the deuterated latex particles used to prepare the film.

$$d = R_g(t) - R \tag{4}$$

These authors found that d scales as expected for $X(t)$ in planar systems, namely, that d increased as $t^{1/4}$ at early times, and as t approached T_{rep}, crossed over to a $t^{1/2}$ dependence. This result suggests that the scaling relationship predicted for the planar geometry carries over to spherical diffusion. On the other hand, the crossover in d took place for a value of d smaller than the radius of gyration R_G of the individual polymer chains in the sample. The authors comment that this difference may be related to the way in which d was calculated. Analyzing data in terms of eq 4 is tantamount to imposing a hard-sphere model on the shape of the deuterated domain throughout the diffusion process. As Wool emphasizes,[6] the fuzzy interface generated by diffusion is best described as a mass fractal. The authors explain that if the same R_g values are interpreted in terms of a mass fractal, the corresponding radii of interpenetration are larger.

From the discussion above, we see that the SANS experiment provides data sensitive to the average penetration distance d, whereas the data from the FRET experiment monitors the number of monomers $N(t)$ that diffuse across the original interface. Other more subtle features differ in the two experiments. The most important is that the FRET experiment is much more sensitive to changes that occur at the earliest stages of the diffusion process. A simple argument emphasizes this point. In terms of the hard-sphere model, an increase in d of 10% is perhaps the lower limit of change that can be detected in the SANS experiment. This small change in d corresponds to a 30% increase in the sphere volume. For our specific experiment, a 10% increase in the cell radius (Chart 1) corresponds to a mass transfer value of $f_s = 0.3$ and a fraction of mixing $f_m = 0.4$.[14] An increase of this radius by 20% corresponds to an $f_s = 0.7$ and $f_m \approx 1$. Thus, the ET experiment provides a large change in signal for diffusion lengths that cause only small changes in SANS scattering profile. The SANS experiment provides high-quality data for diffusion over larger distances and continues to provide information about diffusion over length scales larger than that of the cell diameter.

From this perspective, we can understand the absence of a second crossover in the FRET experiment back to the $t^{1/2}$ dependence predicted for Fickian diffusion at $t > T_{rep}$. This diffusion should occur over distances larger than the radius of gyration of the diffusing chains. For PBMA of $M_w = 4 \times 10^5$, R_G can be estimated to be 13 nm.[29] An increase in radius of 13 nm for a particle with $R = 60$ nm corresponds to an 80% increase in volume. Even if the FRET experiment were sensitive to this crossover, it would only appear in the data at f_m values approaching 1. To search for this crossover, one would have to carry out new experiments with particles with a much larger diameter, so that a 13 nm increase in radius would correspond to a much smaller increase in the extent of mixing.

Polydispersity Effects (SANS). Molecular weight distribution (MWD) also has an important influence on the interdiffusion experiment. From a theoretical perspective, the effect of MWD on polymer dynamics at interfaces was examined by Tirrell[30] and by Wool.[6] By assuming independent chain diffusion, the contributions to the concentration profile from individual reptating chains can be determined for any molecular weight distribution.[6] At a given interdiffusion time, part of the polymer chains will have already reached their equilibrium state (their chain conformation is Gaussian; their interdiffusion time $t > T_{rep}$), while the longer chains are still in their nonequilibrium state. Returning to the experiment, we see that this approach can in principle be used to generate a model concentration profile that can be used to interpret individual scattering intensity or fluorescence decay curves.

It is much more difficult to understand the influence of MWD on the data when one interprets the scattering experiment in terms of a Guinier analysis or a FRET experiment in terms of the change in Φ_{ET}. Hahn et al.,[10b] for example, commented that in a SANS experiment on a latex film containing a distribution of molecular weights, the smearing effect of short chains may affect the neutron scattering intensity for samples annealed for relatively long times. In a review article, Sperling

et al.[31] compared the time profile of d for two PS films of similar molecular weights but very different MWD. The data for the monodisperse sample with M_w = 189 000 are those reported by Kim et al.[28] cited above obtained for films formed with the artificial PS latex particles, with a $t^{1/4}$ dependence crossing over to a $t^{1/2}$ dependence for times greater than T_{rep}. In contrast, the results of Yoo et al.[32] for films formed from latex particles synthesized by emulsion polymerization (with M_n = 69 000, M_w = 250 000) gave a linear plot of log d vs log t, with a slope intermediate between $^1/_4$ and $^1/_2$. For experiments carried out at the same temperature, diffusion was substantially faster for the sample of narrow molecular weight distribution.

Polydispersity Effects (FRET). Farinha et al.[33] and Liu et al.[34] used simulations of the FRET experiment, coupled with experimental results, to try to understand how a distribution of diffusing species affects the signal one obtains. They showed that if the distribution of diffusing species is not too large, an individual $I_D(t')$ fluorescence decay trace for a sample subjected to a certain annealing time can be fitted in terms of a single average (Fickian) diffusion coefficient D_{av}. As the diffusion time increased, they could still fit each decay trace with a single D_{av} value, but the magnitude of D_{av} decreased as the extent of diffusion proceeded. When the distribution of diffusing species is too broad, this approach fails. Here it is possible to input a distribution of D_s values based, for example, on the independently determined MWD.[34] While these simulations teach us something about the FRET experiment, they cannot provide us with quantitative information about the polymer diffusion without a proper model of the diffusion process itself.

What we learn from these simulations is how the distribution of species with different molecular weights contributes to the measured signal in a FRET experiment analyzed in terms of Φ_{ET}. The D-labeled polymers of highest diffusivity make early time contributions to the growth of f_m. These polymers quickly become fully mixed with A-labeled polymers. Irrespective of their subsequent diffusion in the system, they make a constant contribution to the measured extent of energy transfer. If a latex sample contains both low-M polymer for which melt diffusion follows Fick's law and high-M polymer for which entanglements impede diffusion, the diffusion of the former would dominate the early time signal and lead to a $t^{1/2}$ increase in f_m, as we found in our sample for $f_m < 0.2$. Subsequently, the ET signal due to this polymer would remain a constant in the background. The subsequent growth in f_m would be sensitive to the mass transfer governed by reptation diffusion, as influenced by the polydispersity of the polymer sample.

Location of the Chain Ends. The final point to address concerns the location and the nature of the polymer chain ends with respect to the interfaces in a latex film. One imagines that groups at the surface of the latex particles in the aqueous dispersion remain at the interface when the particles deform and pack into a dense film. Thus, one needs information about the location and nature of the ends of the polymer molecules that make up the latex particles.

Polymers prepared by emulsion polymerization often contain initiator groups at the chain ends. The fraction of polymers bearing these groups depends on the termination mechanism and the importance of chain transfer in controlling the polymer molecular weight. We use persulfate as the initiator, which introduces $-OSO_3^-$ groups on the polymer chain end. To obtain low molecular weight emulsion polymers, we add a chain transfer agent to the reaction medium. For the synthesis of the PBMA latex with M_w = 34 000, most of the polymer molecules do not have polar end groups and are unlikely to be concentrated at the particle surface. In the synthesis of the high-M sample (see Table 2) no chain transfer agent was employed. Their polar end groups tend to segregate to the particle surface, where they can be detected by titration of the latex when it is dispersed in water.[35] As a consequence, it is likely that the ends of these chains will be found near the intercellular interface in the newly formed latex films. The presence of polar end groups may explain the lower diffusion rates found by the Lehigh group for PS prepared by emulsion polymerization compared to that for miniemulsified polystyrene.

The scaling exponent for penetration depth does not change for a system in which the chain ends segregate to the surface, whereas $N(t)$ is now predicted to increase as $t^{1/2}$. The SANS experiment is not sensitive to the issue of the spatial distribution of the chain ends. The FRET experiment should be sensitive to this distribution, and we expected to find a value consistent with or intermediate between the predicted values of $^3/_4$ (uniform) and $^1/_2$ (segregated) for different chain end distributions. What we find, and cannot as yet explain, is that f_m for the high molecular weight sample increases as $t^{1/4}$.

Summary

We have compared experiments in which we monitored the growth in energy transfer efficiency due to polymer diffusion in PBMA latex films for two sets of polymers. In the first set of experiments, the low-M sample has M_w = 34 000, close to the entanglement molecular weight ($M_e \approx$ 30 000) for PBMA. Its polymer diffusion follows Fick's law with the growth in f_m scaling with $t^{1/2}$. In the second set of experiments, involving polymer with M_w = 380 000 ($M_w > 10M_e$), we observe a change in the time dependence of f_m. At early times, for values of $f_m < 0.2$, f_m scales as $t^{1/2}$. There is a sharp crossover to a $t^{1/4}$ scaling relationship for values of $f_m > 0.2$. The most likely explanation of the early-time behavior is Fickian diffusion of the lowest molecular weight components of the broadly disperse polymer molecular weight (M_w/M_n = 3). The scaling of f_m with $t^{1/4}$ does not appear to be consistent with the predictions of the theory of polymer diffusion across interfaces. The parameter f_m is a measure of the number of monomers crossing the interface. For diffusion across a planar interface $N(t)$ is predicted to increase as $t^{3/4}$ if the chain ends are uniform and as $t^{1/2}$ if they are segregated to the interface.

Acknowledgment. The authors thank ICI, ICI Canada, and NSERC Canada for their support of this research.

References and Notes

(1) Doi, M.; Edwards, S. F. *The Theory of Polymer Dynamics*; Oxford University Press: Oxford, England, 1986.
(2) de Gennes, P. G. *Scaling Concepts in Polymer Physics*; Cornell University Press: Ithaca, NY, 1979.
(3) de Gennes, P. G. *C. R. Seances Acad. Sci., Ser. 2* **1981**, *292*, 1505. de Gennes, P. G. *J. Chem. Phys.* **1980**, *72*, 4756. de Gennes, P. G. *C. R. Acad. Sci., Ser. 2* **1988**, *307*, 1841.

(4) Prager, S.; Tirrel, M. *J. Chem. Phys.* **1981,** 5194.
(5) Wool, R. P.; O'Connor, K. M. *J. Appl. Phys.* **1981**, *52*, 5953. Wool, R. P.; O'Connor, K. M. *J. Polym. Sci., Polym. Lett. Ed.* **1982**, *20*, 7.
(6) Wool, R. P. *Polymer Inerfaces;* Hanser Publishers: Munich, 1995.
(7) Crank, J. *The Mathematics of Diffusion*; Clarendon: Oxford, UK, 1974.
(8) (a) Whitlow, S. J.; Wool, R. P. *Macromolecules* **1991**, *24*, 5926. (b) Zheng, X.; Sauer, B. B.; Van Alsten, J. G.; Schwarz, S. A.; Rafailovich, M. H.; Sokolov, J.; Rubinstein, M. *Phys. Rev. Lett.* **1995**, *74*, 407.
(9) (a) Russell, T. P.; Karin, A.; Mansour, A.; Felcher, G. P. *Macromolecules* **1988**, *21*, 1890. (b) Composto, R. J.; Stein, R. S.; Kramer, E. J.; Jones, R. A. L.; Mansour, A.; Karin, A.; Felcher, G. P. *Macromolecules* **1989**, *156*−*157*, 434.
(10) (a) Hahn, K.; Ley, G.; Schuller, H.; Oberthur, R. *Colloid Polym. Sci.* **1986**, *264*, 1092. (b) Hahn, K.; Ley, G.; Oberthur, R. *Colloid Polym. Sci.* **1988**, *266*, 631.
(11) (a) Mohammadi, N.; Yoo, J. N.; Klein, A.; Sperling, L. H. *J. Polym. Sci., Part B: Polym. Phys.* **1992**, *30*, 1311. (b) Mohammadi, N.; Kim, K. D.; Klein, A.; Sperling, L. H. *J. Colloid Interface Sci.* **1993**, *157*, 124. (c) Mohammadi, N.; Klein, A.; Sperling, L. H. *Macromolecules* **1993** *26*, 1019.
(12) Kim, K. D.; Sperling, L. H.; Klein, A.; Wignall, G. D. *Macromolecules* **1993**, *26*, 4624.
(13) Joanicot, M.; Wong, K.; Cabane, B. *Macromolecules* **1996**, *29*, 4976.
(14) Farinha, J. P. S.; Martinho, J. M. G.; Yekta, A.; Winnik, M. A. *Macromolecules* **1995**, *28*, 6084.
(15) Dhinojwala, A.; Torkelson, J. M. *Macromolecules* **1994**, *27*, 4817. Liu, Y. S.; Feng, J.; Winnik, M. A. *J. Chem. Phys.* **1994**, *101*, 9096. Kim, H.-B.; Winnik, M. A. *Macromolecules* **1995**, *28*, 2033.
(16) Yekta, A.; Duhamel, J.; Winnik, M. A.*Chem. Phys. Lett.* **1995**, *235*, 119. Farinha, J.; Martinho, J. M. G.; Yekta, A.; Winnik, M. A. *Macromolecules* **1994**, *27*, 1994.
(17) Boczar, E. M.; Dionne, B. C.; Fu, Z.; Kirk, A. B.; Lesko, P. M.; Koller, A. D. *Macromolecules* **1993**, *26*, 5772.
(18) Juhué, D.; Lang, J. *Macromolecules* **1995**, *28*, 1306.
(19) The M_e value for PBMA was estimated according to: Kavassalis, T. A.; Noolandi, J. *Macromolecules* **1989**, *22*, 2709. For an experimental value, see: Porter, R. S.; Johnson, J. F. *Chem. Rev.* **1966**, *66*, 1.
(20) Odrobina, E.; Feng, J.; Pham, H. H.; Winnik, M. A. *Macromolecules* **2001**, *34*, 6039.
(21) Odrobina, E.; Feng, J.; Kawaguchi, S.; Winnik, M. A.; Neag, M.; Meyer, E. F. *Macromolecules* **1998**, *31*, 7239.
(22) O'Connor, D. V.; Phillips, D. *Time-Correlated Single Photon Counting*; Academic Press: London, UK, 1984.
(23) Berlman, I. B. *Energy Transfer Parameters of Aromatic Compounds*; Academic Press: New York, 1973.
(24) Feng, J.; Pham, H.; Stoeva, V.; Winnik, M. A. *J. Polym. Sci., Polym. Phys.* **1998**, *36*, 1129.
(25) (a) Voyutski, S. *J. Polym. Sci., Part A* **1958**, *32*, 528. (b) Voyutski, S. *Autohesion and Adhesion of High Polymers*; Wiley-Interscience: New York, 1963.
(26) Wang, Y.; Zhao, Ch.-L.; Winnik, M. A. *J. Chem. Phys.* **1991**, *95*, 2143.
(27) Ferry, J. D. *Viscoelastic Properties of Polymers*; Wiley: New York, 1980.
(28) Kim, K. D.; Sperling, L. H.; Klein, A.; Hammouda, B. *Macromolecules* **1994**, *27*, 6841.
(29) Brandrup, J.; Immergut, E. H.; Grulke, E. A. *Polymer Handbook*, 4th ed.; Wiley-Interscience: New York, 1999; p VII-50.
(30) Tirrell, M. *Rubber Chem. Technol.* **1984**, *57*, 523.
(31) Sperling, L. H.; Klein, A.; Sambasivam, M.; Kim, D. K. *Polym. Adv. Technol.* **1993**, *5*, 453.
(32) (a) Yoo, J. N.; Sperling, L. H.; Klein, A.; Glinka, C. J. *Macromolecules* **1990**, *23*, 3962. (b) *Macromolecules* **1991**, *24*, 3962.
(33) Farinha, J. P. S.; Martinho, J. M. G.; Kawaguchi, S.; Yekta, A.; Winnik, M. A. *J. Phys. Chem.* **1996**, *100*, 12552.
(34) Liu, Y. S.; Feng, J.; Winnik, M. A. *J. Chem. Phys.* **1994**, *101*, 9096.
(35) Kawaguchi, S.; Yekta, A.; Winnik, M. A. *J Colloid Interface Sci.* **1995**, *176*, 362.

MA0014618